Electrochimica Acta 194 (2016) 454–460

Contents lists available at ScienceDirect

Electrochimica Acta

journal homepage: www.elsevier.com/locate/electacta

Confined ZrO_2 encapsulation over high capacity integrated 0.5Li$[Ni_{0.5}Mn_{1.5}]O_4$·0.5$[Li_2MnO_3$·Li$(Mn_{0.5}Ni_{0.5})O_2]$ cathode with enhanced electrochemical performance

Gyung-Hwan Lee[a], In Hyung Choi[b], Mi Young Oh[c], Sung Ho Park[a], Kee Suk Nahm[b,c,d,*], Vanchiappan Aravindan[e], Yun-Sung Lee[a,*]

[a] Faculty of Applied Chemical Engineering, Chonnam National University, Gwang-ju 500-757, Republic of Korea
[b] Department of Energy Storage and Conversion Engineering, Jeonju 561-756, Republic of Korea
[c] R&D Education Center for Fuel Cell Materials & Systems, Jeonju 561-756, Republic of Korea
[d] School of Chemical Engineering, Chonbuk National University, Jeonju 561-756, Republic of Korea
[e] Energy Research Institute @ NTU (ERI@N), Nanyang Technological University, Research Techno Plaza, 50 Nanyang Drive, Singapore 637553

ARTICLE INFO

Article history:
Received 4 January 2016
Received in revised form 12 February 2016
Accepted 19 February 2016
Available online 23 February 2016

Keywords:
Integrated electrodes
ZrO_2 coating
high capacity
elevated temperature

ABSTRACT

Confined ZrO_2 encapsulation over high capacity spinel-layer-layer structured 0.5Li$[Ni_{0.5}Mn_{1.5}]O_4$·0.5 $[Li_2MnO_3$·Li$(Mn_{0.5}Ni_{0.5})O_2]$ with various concentration by sol-gel process is reported. Presence of homogeneous ZrO_2 layer is evident from the TEM studies. Various electrochemical studies such as optimization of ZrO_2 concentration followed by rate performance, elevated temperature studies, and potential windows are also performed. Among the studies, 1 wt.% ZrO_2 modification is found superior in 2 – 4.9 V *vs.* Li region compared to rest of the coating concentration and pristine compound. Cyclic voltammetry and impedance studies are also performed to understand the reaction mechanism and other electrochemical aspects.

1. Introduction

Development of high energy Li-ion power packs are desperately required to power the zero emission transportation applications like hybrid electric vehicles (HEV) and electric vehicles (EV) [1–3]. To realize the fabrication of high energy Li-ion battery (LIB), a cathode with high working potential and high capacity is needed. Unfortunately, the available and commercialized cathodes like $LiCoO_2$ (~4 V *vs.* Li), $LiMn_2O_4$ (~4 V *vs.* Li), $LiFePO_4$ (~3.4 V *vs.* Li) are exhibiting the practical capacity $<150\ mAh\ g^{-1}$ which is not sufficient to employ them in high energy LIBs. Therefore, intense research activities are carried out to find out appropriate alternate. Recently, the electrode which undergo beyond one electron reaction is proposed, for example, Li_2MSiO_4, where M = Fe, Mn, Co and Ni [4–6]. Generally, orthosilicates exhibits the capacity $>300\ mAh\ g^{-1}$, but, the wider working potential, inherent electrical conductivity and inferior electrochemical activity certainly forbids the possible usage in practical calls. Also, V_2O_5 is one of the widely investigated cathodes for the LIB, which undergoes multiple electron reaction, but severe structural variation and irreversible capacity loss are the major setbacks [7,8]. Also, another important candidate is layered type Li_2MnO_3 ($Li[Li_{1/3}Mn_{2/3}]O_2$) which exhibits the theoretical capacity of ~229 and ~459 $mAh\ g^{-1}$ for one electron and two electron reactions, respectively [9–16]. Unfortunately, the electrochemical activity of Mn^{4+} is found to be inert, but several reports are available on this fascinating cathode. The electrochemical activity of Li_2MnO_3 is mainly ascribed to the following four reasons, (i) Mn site doping with aliovalent transition metal elements which undergo redox reactions, (ii) removal of Li with accompanied oxygen loss (Li_2O), (iii) oxidation of electrolyte solution and subsequent exchange reaction of H^+ and Li^+, and (iv) oxidation of Mn^{3+}, if the defective layered phase is obtained. This Li-rich compositions certainly attracts the researchers with integrated structure like layered-layered (xLiMnO$_3$·(1-x) $LiMn_{0.5}Ni_{0.5}O_2$) and spinel-layered-layered (xLiNi$_{0.5}$Mn$_{1.5}$O$_4$-(1-x) Li_2MnO_3·$LiNi_{0.5}Mn_{0.5}O_4$) [17]. Presence of Li_2MnO_3 or metal doping certainly translates the better structural and electrochemical stability irrespective of either layered $LiMO_2$ or spinel LiM_2O_4 components with wider operating potential [14,18,19]. Amongst, a layered-layered electrode is found promising in terms capacity, but the net energy density is more or less equal to that of layered $LiCoO_2$. Instead of preparing the $LiMn_2O_4$ based spinel-layer-layer

* Corresponding authors.
E-mail addresses: nahmks@jbnu.ac.kr (K.S. Nahm), aravind_van@yahoo.com (V. Aravindan), leeys@chonnam.ac.kr (Y.-S. Lee).

http://dx.doi.org/10.1016/j.electacta.2016.02.129
0013-4686/

compound, Ni-doped spinel compound is found interesting ($LiNi_{0.5}Mn_{1.5}O_4$) in terms of high energy density *via* higher redox potential. In addition, the higher reversible capacity (>200 mAh g^{-1}) is also worth mentioning, apart from the eco-friendliness and low cost. Though, the spinel-layer-layer integrated structure presents decent working potential and capacity, but capacity fading is a prime issue. In this line, we made an attempt to improve the electrochemical activity of the $0.5Li[Ni_{0.5}Mn_{1.5}]O_4{\cdot}0.5[Li_2MnO_3{\cdot}Li(Mn_{0.5}Ni_{0.5})O_2]$ cathode by adopting surface modification, especially by the ZrO_2 coating with various concentrations. The ZrO_2 has been chosen by considering its highest fracture toughness, which forms a fracture-toughened thin-film solid solution near the particle surface. Further, this ZrO_2 layer significantly improves the structural stability which certainly prevents capacity fading during electrochemical cycling [20]. First, the spinel-layer-layer compound is prepared *via* precipitation and characterized. The detailed structural and electrochemical studies are performed and discussed in this paper.

2. Experimental section

The integrated $0.5Li[Ni_{0.5}Mn_{1.5}]O_4{\cdot}0.5[Li_2MnO_3{\cdot}Li(Mn_{0.5}Ni_{0.5})O_2]$ phase was prepared by co-precipitation technique described by un in the previous work. Briefly, carbonate co-precipitation procedure in a continuous stirred tank reactor (CSTR) was employed. For the preparation of $Mn_{0.75}Ni_{0.25}CO_3$ precursor, Mn: Ni ratio was fixed to 3:1 by using analytical grade starting materials like Li_2CO_3, Na_2CO_3, $MnSO_4$, $NiSO_4$, NH_4OH. The Na_2CO_3 solution was used to adjust the pH value. Once the $Mn_{0.75}Ni_{0.25}CO_3$ precipitate occurs, then it was filtered, washed and dried at 100 °C for 12 h in air. The integrated spinel-layer-layer structure was obtained by reacting the obtained carbonate precursor with appropriate amount of Li_2CO_3 *via* solid-state reaction at 650 °C for 5 h, and fired at 900 °C for 12 h in air.

To prepare ZrO_2 coated $0.5Li[Ni_{0.5}Mn_{1.5}]O_4{\cdot}0.5[Li_2MnO_3{\cdot}Li(Mn_{0.5}Ni_{0.5})O_2]$, the acetate salt of zirconium, namely zirconium (IV) acetate hydroxide (Sigma-Aldrich, USA), was first dissolved in distilled water and stirred constantly at 50 °C. The synthesized $0.5Li[Ni_{0.5}Mn_{1.5}]O_4{\cdot}0.5[Li_2MnO_3{\cdot}Li(Mn_{0.5}Ni_{0.5})O_2]$ powders was added to the coating solution, maintaining dynamic stirring for the subsequent 24 h. The final amount of coating materials in the mixture was fixed at 1, 3 and 5 wt.% of the initial starting materials. The mixture was dried at 60 °C and finally fired at 500 °C for 5 h in an air atmosphere. A heating rate of 10 °C $min.^{-1}$ was maintained throughout the synthesis unless specified.

X-ray diffraction (XRD) studies were performed using Rint 1000 Regaku, Japan equipped with Cu Kα radiation for the structural analysis. Morphological studies were performed with field emission scanning electron microscopy (FE-SEM, S4700, Hitachi, Japan). Transmission electron microscopy (TEM, TecnaiF20, Philips, Holland) was also performed to ensure the presence of ZrO_2 layer. All the electrochemical studies were conducted in CR2032 coin-cell configuration. As usual, the test electrodes were fabricated with accurately weighed 20 mg of active material, 3 mg of conductive additive (Ketzen black) and 3 mg of Teflonized acetylene black (TAB-2) using ethanol. This resultant mixture was pressed over 200 mm^2 stainless steel mesh and dried at 160 °C for 4 h in vacuum oven. Test cells were assembled in Ar filled glove box using metallic lithium as counter electrode and it was separated by porous polypropylene separator (Celgard 3401). 1 M $LiPF_6$ ethylene carbonate (EC)/di-methyl carbonate (DMC) (1:1 v/v) was used as electrolyte solution. Galvanostatic charge–discharge studies were carried out in ambient conditions with various potentials windows and current densities.

3. Results and discussion

Fig. 1 represents the XRD pattern of such integrated $0.5Li[Ni_{0.5}Mn_{1.5}]O_4{\cdot}0.5[Li_2MnO_3{\cdot}Li(Mn_{0.5}Ni_{0.5})O_2]$ phase with various concentration of ZrO_2 coatings. It is well known that, both layered and spinel phase materials exhibits the characteristic reflection almost in the same region (~18°). Therefore, other reflections located at ~36.5 and ~44.6° could be used to distinguish the spinel phase from layered one. Similarly, the layered Li_2MnO_3 phase showed a characteristic superstructure at ~22° which is evident with less intensity. This XRD pattern clearly suggests the solid solution formation upon the synthesis. Further, there are no additional peak positions noted after the ZrO_2 modification irrespective of the concentrations used. This indicates that ZrO_2 did not influence the structural properties of the $0.5Li[Ni_{0.5}Mn_{1.5}]O_4{\cdot}0.5[Li_2MnO_3{\cdot}Li(Mn_{0.5}Ni_{0.5})O_2]$ phase prepared and anticipated to be in the surface of the said particulates. Nevertheless, the EDAX mapping and XPS spectra clearly reveal the existence of ZrO_2 layer (Fig. S1).

Morphological studies were performed for ZrO_2 modified integrated $0.5Li[Ni_{0.5}Mn_{1.5}]O_4{\cdot}0.5[Li_2MnO_3{\cdot}Li(Mn_{0.5}Ni_{0.5})O_2]$ phase and given in Fig. 2. FE-SEM picture reveal the presence of sub-micron sized irregular shaped particulates. Also, interconnectivity between the particles is also seen. After the surface modification with ZrO_2, increase in the roughness of the surface

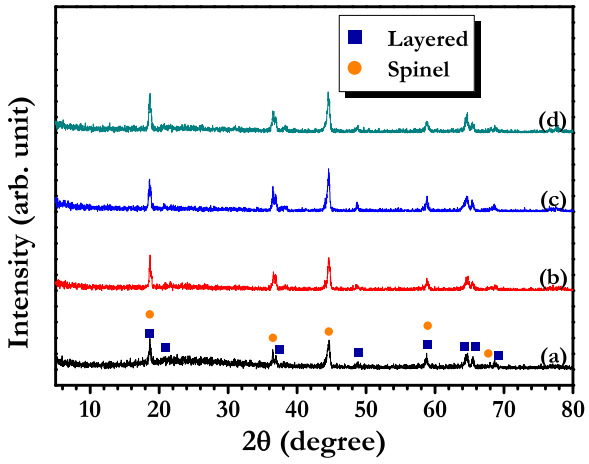

Fig. 1. XRD pattern of $0.5Li[Ni_{0.5}Mn_{1.5}]O_4{\cdot}0.5[Li_2MnO_3{\cdot}Li(Mn_{0.5}Ni_{0.5})O_2]$ with various concentration of ZrO_2 coatings, (a) pristine, (b) 1 wt.%, (c) 3 wt.%, and (d) 5 wt.%.

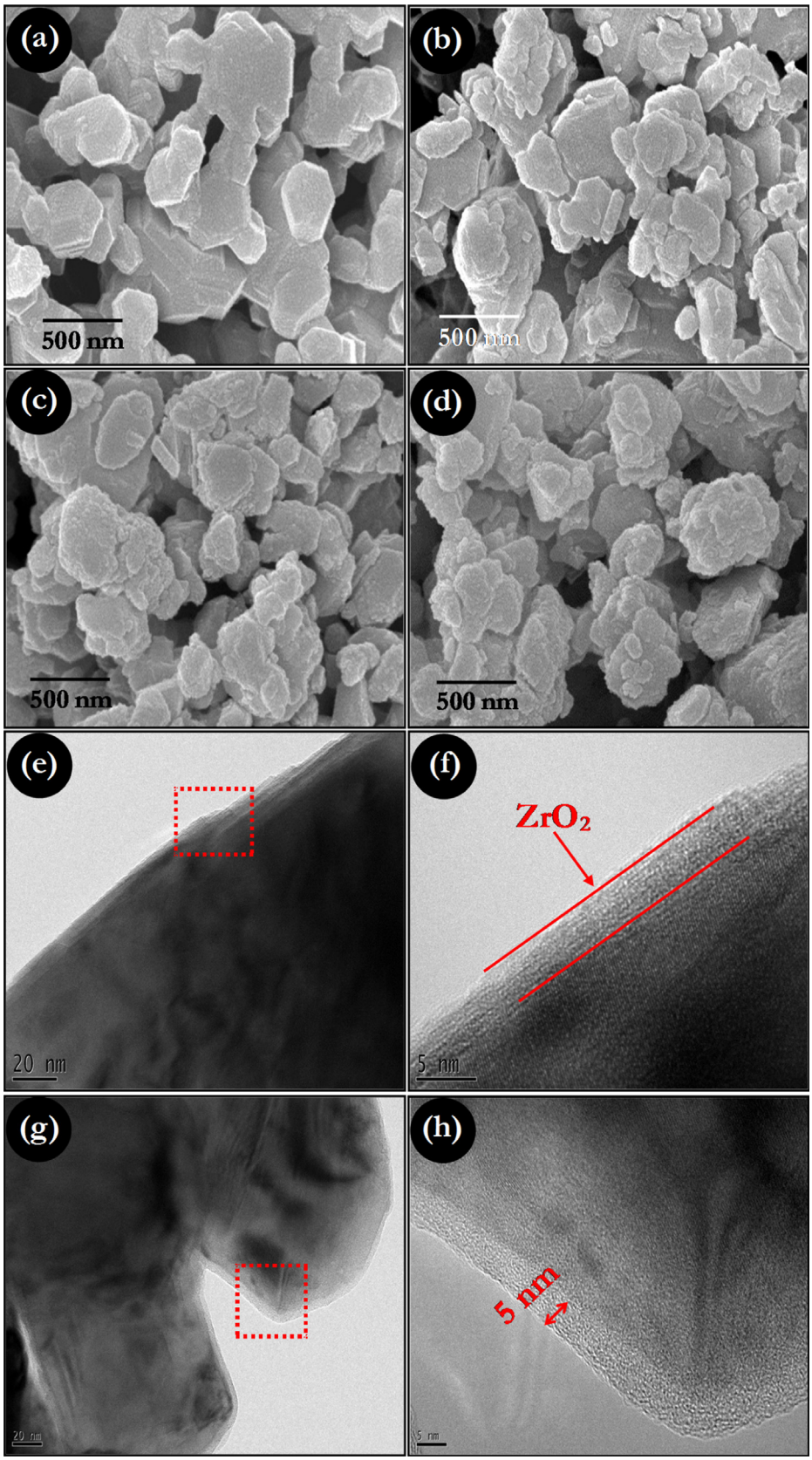

Fig. 2. FE-SEM pictures of $0.5Li[Ni_{0.5}Mn_{1.5}]O_4 \cdot 0.5[Li_2MnO_3 \cdot Li(Mn_{0.5}Ni_{0.5})O_2]$ with various concentration of ZrO_2 coatings, (a) pristine, (b) 1 wt.%, (c) 3 wt.%, and (d) 5 wt.%, TEM images of (e-f) 1 wt.%, and (g-h) 5 wt.%.

is noted irrespective of the loading (Fig. 2b-d). The TEM pictures and it magnified images clearly showed the presence of thin layer of ZrO_2 (Fig. 2e-h). The coating thickness is increased with increasing ZrO_2 loading, for instance more or less 5 nm thick

homogeneous coating layer is seen over the particulates for 5 wt.% modification. This morphologies study clearly inferred that, the ZrO_2 is present on the top of the particles and consistent with the XRD studies which are not influence the structural changes in the parent compound.

Electrochemical performance of integrated $0.5Li[Ni_{0.5}Mn_{1.5}]O_4{\cdot}0.5[Li_2MnO_3{\cdot}Li(Mn_{0.5}Ni_{0.5})O_2]$ cathode at various loadings of ZrO_2 in half-cell configurations were carried out between 2–4.9 V *vs.* Li at current density of 0.1 mA cm^{-2} and given in Fig. 3. It is obvious to note that during the discharge process, the small plateau around ~4.7 V *vs.* Li is associated with the reduction of $Ni^{4+/2+}$ in spinel compound, $Li[Ni_{0.5}Mn_{1.5}]O_4$ [21] and the appearance of monotonous curves ~4 V *vs.* Li is correlated to the $Ni^{4+/2+}$ redox reaction in layered compound, $Li(Mn_{0.5}Ni_{0.5})O_2$. Finally, the very small short plateau ~2.7 V *vs.* Li is corresponds to the octahedral Li-insertion/extraction in spinel compound [22,23]. On the other hand, upon charge process, the presence of long distinct plateau ~4.5 V *vs.* Li is corresponds to the activation of layered compound Li_2MnO_3 by removal of Li along with oxygen (Li_2O) [13]. The discharge capacity of ~202, ~234, ~230 and ~231 mAh g^{-1} is observed for the coating concentration of 0, 1, 3 and 5 wt.% of ZrO_2 modification, respectively. Apparently, notable improvements from the discharge capacity are noted after the ZrO_2 modification. However, there is no obvious difference between the capacities is noted for different loading of ZrO_2. Therefore, galvanostatic studies are extended to 50 cycles and the corresponding profiles are given in Fig. 3b. The half-cells rendered, ~84, ~80, ~77 and ~74% of initial capacity for 0, 1, 3 and 5 wt.% of ZrO_2 modification, respectively. Although, pristine electrodes displayed higher capacity retention characteristics, but certainly the reversible capacity is lower (~171 mAh g^{-1}) compared to 1 wt.% ZrO_2 loading (~187 mAh g^{-1}). In order to ensure advantages of ZrO_2 layer over such integrated cathode, a high current performance was conducted. Interestingly, all the ZrO_2 modified electrodes displayed good cycling profiles with reversibility except unmodified one (Fig. S2). From these studies, it is clear that, small amount of coating layer is sufficient to provide the desired improvement in the electrochemical activity. Increasing concentration leads to impede the electrochemical activity of electrode owing to the insulating nature of the material. Nevertheless, the presence of ZrO_2 certainly prevents unwanted side reaction with electrolyte counterpart which in turn provides the improved capacity profiles compared to bare electrode [20].

To understand the reaction mechanism and conducting profiles of such ZrO_2 modified electrodes, CV and impedance studies were performed and given in Fig. 4. CV traces for such integrated electrodes in first cycle is compared for all the concentrations and given in Fig. 4a. It is worth mention that different ZrO_2 loading exhibits almost same peak current, except the pristine material. This suggests that $0.5Li[Ni_{0.5}Mn_{1.5}]O_4{\cdot}0.5[Li_2MnO_3{\cdot}Li(Mn_{0.5}Ni_{0.5})O_2]$ showed a negligible difference between the capacity profiles irrespective of the ZrO_2 concentration, which is clearly consistent with galvanostatic profiles. The CV profile for pristine materials is entirely different than ZrO_2 modified cathodes in the first cycle, but remains same after the first cycle (Fig. S3). The presence of sharp peaks ~3 V *vs.* Li is associated with octahedral sites of spinel component, $Li[Ni_{0.5}Mn_{1.5}]O_4$ and a broader peak potential located at ~4 V *vs.* Li corresponds to the layered $Li(Mn_{0.5}Ni_{0.5})O_2$ phase. The appearance of high intense peak at ~4.7 V *vs.* Li is associated with $Ni^{2+/4+}$ redox reaction of spinel component and the activation of layered Li_2MnO_3 cannot be ruled out. The observed peak positions are consistent with the galvanostatic measurements. Impedance spectra has been recorded for all the freshly assembled cells and given in Fig. 4b. The impedance spectra composed of three main parts, the high frequency region (R_S, solution resistance), medium frequency region (R_{CT}, charge transfer resistance) and low frequency region *i.e.,* inclined at 45° (Z_W, Warburg tail). The ZrO_2 modification certainly improves the electrical conductivity and also, effectively prevents the unwanted side reaction with the electrolyte counterpart which eventually reflects in the enhancement in the capacity profile [4,24]. As expected, pristine electrode showed higher R_{CT} (~96 Ω) values compared to and ZrO_2 modified electrodes which offered less resistance, for example, ~60, ~62, and ~72 Ω for 1, 3 and 5 wt.% loadings, respectively. However, the negligible variation of the R_{CT} is observed irrespective of the ZrO_2 concentration, except 5 wt.%, which is consistent with the galvanostatic cycling. Also, the variation in the cell impedance is consistent with the LiF/FeF_3 protective layer over Li-rich cathodes [25]. High concentration (5 wt.%) ZrO_2 modification tends to the

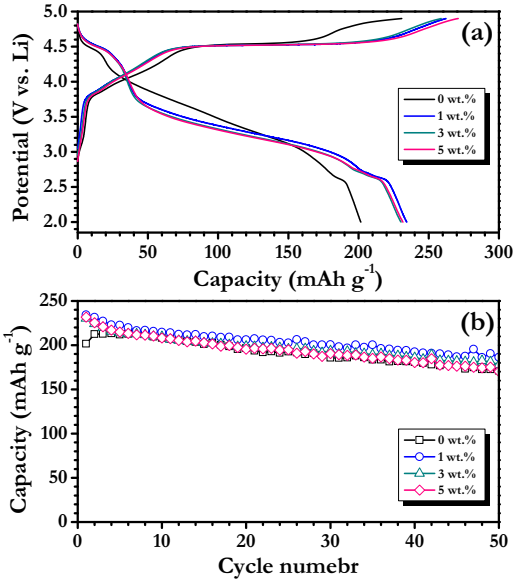

Fig. 3. Electrochemical performance of $0.5Li[Ni_{0.5}Mn_{1.5}]O_4{\cdot}0.5[Li_2MnO_3{\cdot}Li(Mn_{0.5}Ni_{0.5})O_2]$ with various concentration of ZrO_2 coatings (a) charge-discharge curves, and (b) plot of discharge capacity *vs.* cycle number.

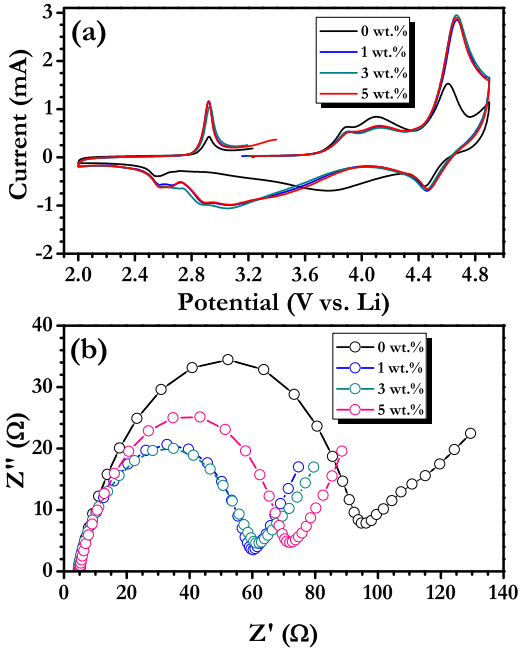

Fig. 4. (b) Cyclic voltammetric traces of ZrO_2 coated $0.5Li(Mn_{1.5}Ni_{0.5})O_4$-$0.5[Li_2MnO_3{\cdot}Li(Mn_{0.5}Ni_{0.5})O_2]$ electrodes recorded in half cell configuration between 2.0–4.9 V *vs.* Li at slow scan rate of 0.1 mV s^{-1} in room temperature at various concentrations, and (b) electrochemical impedance spectra of at various ZrO_2 loadings.

thicker modification and hampers the ion migration which is clearly evident from the drastic increase in the R_{CT} resistance.

Elevated temperature performance (55 °C) is one of the important parameter to be studied for such high capacity cathodes and given in Fig. 5. For the high temperature performance, only pristine, low and high level of ZrO_2 loading has been conducted. Generally, increase in temperature tends to increase in electrical conductivity which in turn improved reversibility is noted during the galvanostatic measurements. Accordingly, the reversible capacity of ~254, ~255, and ~249 mAh g^{-1} is observed for pristine, 1 and 5 wt.% of ZrO_2 coating, respectively. Though, there is no much difference between the initial reversibility is noted, but the cycleability is the important aspect. Accordingly, ZrO_2 modification renders ~81 and ~43% initial reversibility after 28 cycles for 1 and 5 wt.% loadings, respectively. At elevated conditions, the PF_6^- anions are highly accelerated and vigorously reacts the trace amount of moisture which produces HF and PF_5 [26]. This certainly leads to the unwanted side reaction with electrolyte component *i.e.* HF reacts with both transition metal and cation and later, destroys it. Finally, the severe deterioration occurs on the cathodic performance. On the other hand, presence of surface layer hampers such unwanted reaction and maintains the electrochemical activity of the cathode, especially in high temperature conditions. Interestingly, 1 wt.% coated electrodes showed good performance compared to the 5 wt.% modification and we found that, 1 wt.% ZrO_2 modification is sufficient to provide good stability without compromising the reversibility. In contrary, there is no obvious difference between the electrochemical profiles is noted when increasing the current rate to 1C. This is mainly because of the limited Li-ion kinetics at high current rates, which allows surface of the active material in electrochemical reaction. As a result, improved cycleability is noted for all the cases (Fig. S2).

Similar to elevated temperature performance, rate capability is also an important to evaluate. Therefore, rate performance studies are conducted for the pristine and 1 wt.% ZrO_2 modified $0.5Li[Ni_{0.5}Mn_{1.5}]O_4{\cdot}0.5[Li_2MnO_3{\cdot}Li(Mn_{0.5}Ni_{0.5})O_2]$cathodes and given in Fig. 6. As observed earlier, increase in capacity profile is noted for pristine electrode, whereas marginal decrease in capacity profiles are evident for 1 wt.% ZrO_2 modified one. Interestingly, the obvious difference between the electrochemical performances is evident at low current rates only. At higher rates, the surface of the active material only involves the reaction, hence, there is no much

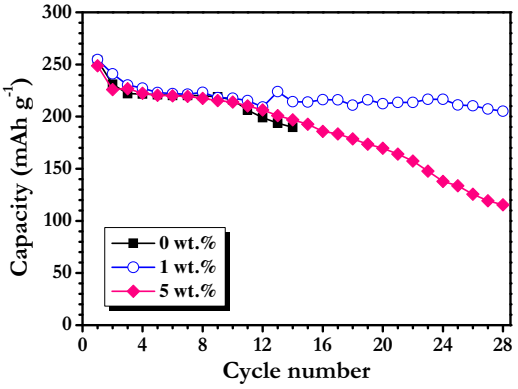

Fig. 5. Electrochemical performance of $0.5Li[Ni_{0.5}Mn_{1.5}]O_4{\cdot}0.5[Li_2MnO_3{\cdot}Li(Mn_{0.5}Ni_{0.5})O_2]$ with various concentration of ZrO_2 coatings (0, 1 and 5 wt. %).

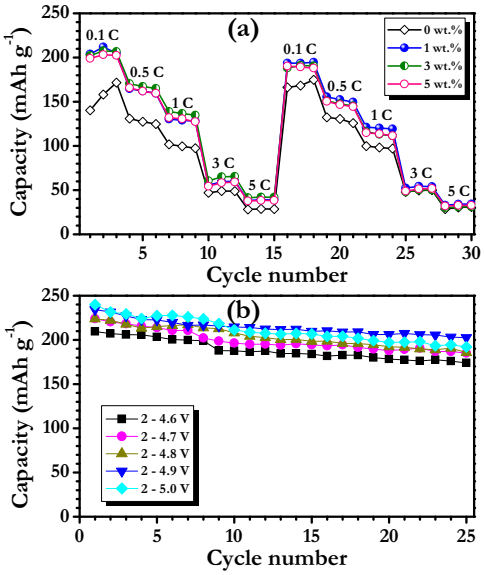

Fig. 6. (a) Electrochemical performance of $0.5Li[Ni_{0.5}Mn_{1.5}]O_4{\cdot}0.5[Li_2MnO_3{\cdot}Li(Mn_{0.5}Ni_{0.5})O_2]$ modified with various ZrO_2 concentrations at various current densities, and (b) Plot of discharge capacity *vs.* cycle number for ZrO_2 (1 wt.%) modified $0.5Li[Ni_{0.5}Mn_{1.5}]O_4{\cdot}0.5[Li_2MnO_3{\cdot}Li(Mn_{0.5}Ni_{0.5})O_2]$ at various testing potential at current density of 0.1 mA cm^{-1}.

difference between pristine and 1 wt.% coated electrodes. In addition to the rate performance analysis, testing potential also plays an important role in the activation and electrochemical performance of Li_2MnO_3 based cathodes. In this line, we tested the ZrO_2 modified $0.5Li[Ni_{0.5}Mn_{1.5}]O_4{\cdot}0.5[Li_2MnO_3{\cdot}Li(Mn_{0.5}Ni_{0.5})O_2]$ (1 wt.%) cathodes at various potential windows to study the stability and reversible capacity (Fig. S4). At 4.6 V *vs.* Li window, contribution from the spinel compound, is limited, since the $Ni^{2+/4+}$ redox reaction occurs at ~4.7 V *vs.* Li which results the less reversible capacity (~210 mAh g^{-1}). Accordingly, as expected, at 5 V *vs.* Li testing window translates higher reversible capacity (~240 mAh g^{-1}), but the capacity fading is found severe compared to the ~4.9 V *vs.* Li window. This study clearly suggests the 2–4.9 V *vs.* Li is optimum to achieve high performance in terms of reversibility and cycleability. Further studies are in progress to improve the electrochemical activity by adopting conductive coatings especially carbonaceous materials.

4. Conclusion

We successfully demonstrated the improvement in electrochemical activity of integrated spinel-layer-layered compound, $0.5Li[Ni_{0.5}Mn_{1.5}]O_4{\cdot}0.5[Li_2MnO_3{\cdot}\ Li(Mn_{0.5}Ni_{0.5})O_2]$ after the ZrO_2 modification with various concentrations. Amongst, 1 wt.% modification delivered better battery performance in terms of high reversibility, cycleability, and high temperature performance. Various potential windows were also investigated to ensure the optimal region to yield high performance. First, the integrated phase was obtained by carbonate precipitation technique and followed by ZrO_2 modification with sol-gel process. The presence of ZrO_2 layer over such integrated cathodes was confirmed by TEM analysis.

Acknowledgements

This research was supported by Basic Science Research Program through the National Research Foundation of Korea(NRF) funded by the Ministry of Education(No. 2013R1A1A2012656).

Appendix A. Supplementary data

Supplementary data associated with this article can be found, in the online version, at http://dx.doi.org/10.1016/j.electacta.2016.02.129.

References

[1] M.M. Thackeray, C. Wolverton, E.D. Isaacs, Energy & Environmental Science 5 (2012) 7854–7863.
[2] V. Aravindan, J. Gnanaraj, Y.-S. Lee, S. Madhavi, Journal of Materials Chemistry A 1 (2013) 3518–3539.
[3] E.J. Cairns, P. Albertus, Annual Review of Chemical and Biomolecular Engineering 1 (2010) 299–320.
[4] V. Aravindan, K. Karthikeyan, K.S. Kang, W.S. Yoon, W.S. Kim, Y.S. Lee, Journal of Materials Chemistry 21 (2011) 2470–2475.
[5] V. Aravindan, K. Karthikeyan, S. Ravi, S. Amaresh, W. Kim, Y. Lee, Journal of Materials Chemistry 20 (2010) 7340–7343.
[6] V. Aravindan, K. Karthikeyan, J. Lee, S. Madhavi, Y. Lee, Journal of Physics D: Applied Physics 44 (2011) 152001.
[7] Y.L. Cheah, V. Aravindan, S. Madhavi, ACS Applied Materials & Interfaces 5 (2013) 3475–3480.
[8] Y.L. Cheah, N. Gupta, S.S. Pramana, V. Aravindan, G. Wee, M. Srinivasan, Journal of Power Sources 196 (2011) 6465–6472.
[9] P. Rozier, J.M. Tarascon, Journal of The Electrochemical Society 162 (2015) A2490–A2499.
[10] H. Yu, H. Zhou, The Journal of Physical Chemistry Letters 4 (2013) 1268–1280.
[11] M.M. Thackeray, C.S. Johnson, J.T. Vaughey, N. Li, S.A. Hackney, Journal of Materials Chemistry 15 (2005) 2257–2267.
[12] A. Manthiram, J.C. Knight, S.-T. Myung, S.-M. Oh, Y.-K. Sun, Advanced Energy Materials 6 (2016) 1501010.
[13] A.D. Robertson, P.G. Bruce, Chemical Communications 0 (2002) 2790–2791.
[14] N. Yabuuchi, K. Yoshii, S.-T. Myung, I. Nakai, S. Komaba, Journal of the American Chemical Society 133 (2011) 4404–4419.
[15] J. Hong, H. Gwon, S.-K. Jung, K. Ku, K. Kang, Journal of The Electrochemical Society 162 (2015) A2447–A2467.
[16] C.S. Yoon, M.H. Choi, B.-B. Lim, E.-J. Lee, Y.-K. Sun, Journal of The Electrochemical Society 162 (2015) A2483–A2489.
[17] C.S. Johnson, N. Li, J.T. Vaughey, S.A. Hackney, M.M. Thackeray, Electrochemistry Communications 7 (2005) 528–536.
[18] M.M. Thackeray, S.-H. Kang, C.S. Johnson, J.T. Vaughey, R. Benedek, S.A. Hackney, Journal of Materials Chemistry 17 (2007) 3112–3125.
[19] I. Hyung Choi, J. Min Choi, Y. Ju Hwang, V. Aravindan, Y. Sung Lee, K. Suk Nahm, Ceramics International 40 (2014) 13033–13039.
[20] C. Li, H.P. Zhang, L.J. Fu, H. Liu, Y.P. Wu, E. Rahm, R. Holze, H.Q. Wu, Electrochimica Acta 51 (2006) 3872–3883.
[21] N. Arun, V. Aravindan, S. Jayaraman, N. Shubha, W.C. Ling, S. Ramakrishna, S. Madhavi, Nanoscale 6 (2014) 8926–8934.

[22] N. Arun, V. Aravindan, W.C. Ling, S. Madhavi, Journal of Power Sources 280 (2015) 240–245.
[23] N. Arun, A. Jain, V. Aravindan, S. Jayaraman, W. Chui Ling, M.P. Srinivasan, S. Madhavi, Nano Energy 12 (2015) 69–75.
[24] J. Fan, G. Li, D. Luo, C. Fu, Q. Li, J. Zheng, L. Li, Electrochimica Acta 173 (2015) 7–16.
[25] T. Zhao, L. Li, R. Chen, H. Wu, X. Zhang, S. Chen, M. Xie, F. Wu, J. Lu, K. Amine, Nano Energy 15 (2015) 164–176.
[26] V. Aravindan, J. Gnanaraj, S. Madhavi, H.-K. Liu, Chemistry –A European Journal 17 (2011) 14326–14346.